

A general numerical analysis of time-domain NQR experiments

Elad Harel ^{a,*}, Herman Cho ^b

^a *Department of Chemistry, University of California, Berkeley, CA 94720, USA*

^b *Fundamental Science Directorate, MS K8-98, Pacific Northwest National Laboratory, Richland, WA 99352, USA*

Received 13 March 2006; revised 27 June 2006

Available online 25 September 2006

Abstract

We introduce a general numerical approach for solving the Liouville equation of an isolated quadrupolar nuclide that can be used to analyze the unitary dynamics of time-domain NQR experiments. A numerical treatment is necessitated by the dimensionality of the Liouville space, which precludes analytical, closed form solutions for $I > 3/2$. Accurate simulations of experimental nutation curves, forbidden transition intensities, powder and single crystal spectra, and off-resonance irradiation dynamics can be computed with this method. We also examine the validity of perturbative approximations where the signal intensity of a transition is proportional to the transition moment between the eigenstates of the system, thus providing a simple basis for determining selection rules. Our method allows us to calculate spectra for all values of the asymmetry parameter, η , and sample orientations relative to the coil axis. We conclude by demonstrating the methodology for calculating the response of the quadrupole system to amplitude- and frequency-modulated pulses.

© 2006 Elsevier Inc. All rights reserved.

Keywords: Time-domain nuclear quadrupole resonance; Time-dependent perturbation theory; Liouville equation

1. Introduction

Nuclear quadrupole resonance (NQR) spectroscopy is a valuable method for probing electronic structure around quadrupolar nuclei in solids [1]. Early theoretical treatments of NQR experiments were based on stationary perturbation theory [1–3] and were unsuited for describing later techniques that made use of coherent excitation and detection schemes. One of the first reports to analyze NQR experiments in the time domain was that of Pratt et al. [4], who obtained exact solutions for the response of an $I = 3/2$ spin to on- and off-resonance pulsed excitation. With their explicit expressions at hand, subsequent workers were able to develop ways of determining the electric field gradient (EFG) tensor from 2D nutation experiments and other methods [5–7]. More recently, Xia et al. [8,9] and Lee [10] have proposed a description of time

domain NQR experiments of $I = 1$ and $3/2$ nuclides in terms of a fictitious spin-1/2 formalism.

Nuclides with $I > 3/2$ present greater mathematical difficulties, and in past treatments the analysis of dynamics has been simplified by assuming that the excitation pulses are selective for only a single transition [11–15]. However, closed form expressions for experimental observables involve complex derivations, even for the most basic experiments in the on-resonance, selective pulse limit. The selective pulse approximation also has the shortcoming that it explicitly ignores the possibility of multi-transition excitations, as might occur for degenerate transitions or broadband excitation pulses. This complication does not arise when $I \leq 3/2$ since the NQR spectra in these cases consist of only a single doubly degenerate line.

Insofar as closed form expressions for NQR observables can be difficult to derive and have been limited thus far to simplified examples, numerical solutions of the Liouville equation are an appealing alternative for obtaining useful results without resorting to restrictive assumptions about the resonance offset, selectivity of the excitation pulses, or symmetry of the EFG tensor. While sophisticated

* Corresponding author. Fax: +1 510 486 5744.
E-mail address: elharel@berkeley.edu (E. Harel).

computational methods have been developed for simulating high-field NMR experiments [16,17], numerical solutions are not as straightforward to formulate for cases where there is no dominant Zeeman interaction to define an axis of quantization. Whether a numerical or analytical approach is taken, the usual starting point for integrating the equations of motion when there are time-varying fields is to identify an interaction representation wherein all time-dependent terms in the Hamiltonian can be neglected because they have high frequencies and are non-resonant, leaving only a static Hamiltonian. In this paper, we introduce an interaction representation that proves to be particularly convenient for accurate numerical calculations. We demonstrate with examples that this approach can be used to treat problems that have been troublesome for analytical methods, including the calculation of off-resonance excitation effects, nutation spectra for $I > 3/2$, and transition probabilities (both allowed and forbidden) for nuclides with asymmetric EFG tensors. We also use numerical calculations to consider the validity of approximating NQR transition probabilities with transition moments, with their significantly simpler mathematical forms.

2. Theory

The laboratory frame Hamiltonian of a single quadrupolar nuclide in zero field, interacting with a linearly polarized, amplitude modulated radiofrequency (rf) field, can be written as

$$\mathcal{H}_L = \mathcal{H}_Q + V(t), \quad (1)$$

where \mathcal{H}_Q and $V(t)$ are the quadrupolar and rf interaction terms, respectively. They can be expanded as

$$H_Q = \frac{e^2 q Q}{4I(2I-1)} \left[3I_z^2 - \mathbf{I}^2 + \frac{\eta}{2}(I_+^2 + I_-^2) \right], \quad (2)$$

$$V(t) = -2\omega_1(t) \cos(\omega_{\text{rf}}t + \phi_{\text{rf}}) \mathbf{I} \cdot \mathbf{n}. \quad (3)$$

In Eq. (3), \mathbf{n} represents the direction of the coil axis relative to the EFG principal axis system, and is specified by the longitudinal and azimuthal angles θ and ϕ , respectively. Unlike the high-field case, it is not a valid approximation to neglect the effects of the counter-rotating component of $V(t)$.

By analogy with the rotating frame formalism used to analyze dynamics in high-field NMR spectroscopy [18], we consider integrating the spin's equations of motion in a zero-field interaction representation defined by the operator

$$A_z(\eta) = \sum_{m=-I}^I m |\psi_m(\eta)\rangle \langle \psi_m(\eta)|, \quad (4)$$

where $|\psi_m(\eta)\rangle$ is an eigenstate of the quadrupolar Hamiltonian \mathcal{H}_Q such that $|\psi_m(0)\rangle = |m\rangle$ is the m th eigenstate of I_z . It follows from these definitions that $A_z(0) = I_z$ and

$$\mathcal{H}_Q = \sum_{m=-I}^I \lambda_m(\eta) |\psi_m(\eta)\rangle \langle \psi_m(\eta)|, \quad (5)$$

where $\lambda_m(\eta)$ is the eigenvalue of \mathcal{H}_Q for the $|\psi_m(\eta)\rangle$ eigenstate, and $[\mathcal{H}_Q, A_z(\eta)] = 0$. The Hamiltonian in the interac-

tion representation defined by the unitary operator $U_{\text{IF}}(\eta, t) = \exp[-i\omega_{\text{rf}}A_z(\eta)t]$ is

$$\mathcal{H}_{\text{IF}}(\eta, t) = \mathcal{H}_{Q,\text{IF}}(\eta) + V_{\text{IF}}(\eta, t) \quad (6)$$

with

$$\begin{aligned} \mathcal{H}_{Q,\text{IF}}(\eta) &\equiv U_{\text{IF}}^\dagger(\eta, t) \mathcal{H}_Q U_{\text{IF}}(\eta, t) - \omega_{\text{rf}} A_z(\eta) \\ &= \sum_{m=-I}^I [\lambda_m(\eta) - m\omega_{\text{rf}}] |\psi_m(\eta)\rangle \langle \psi_m(\eta)|. \end{aligned} \quad (7)$$

From Eq. (7), we see that the applied field is resonant with the splitting between two non-degenerate states $|\psi_m(\eta)\rangle$ and $|\psi_n(\eta)\rangle$ when

$$|\lambda_m(\eta) - \lambda_n(\eta)| \approx \omega_{\text{rf}} |m - n|. \quad (8)$$

The rf interaction Hamiltonian in this frame is given by:

$$V_{\text{IF}}(\eta, t) \equiv U_{\text{IF}}^\dagger(\eta, t) V(t) U_{\text{IF}}(\eta, t). \quad (9)$$

Following the high-field rotating frame example, we attempt to eliminate oscillatory terms by approximating $V_{\text{IF}}(\eta, t)$ with a time average

$$\begin{aligned} V_{\text{IF}}(\eta, T) &\approx T^{-1} \int_0^T V_{\text{IF}}(\eta, t') dt' \\ &= \bar{V}_{\text{IF}}(\eta). \end{aligned} \quad (10)$$

A weak, off-resonant rf field cannot induce transitions between two states $|\psi_m(\eta)\rangle$ and $|\psi_n(\eta)\rangle$ if

$$|\lambda_m(\eta) - \lambda_n(\eta)| - \omega_{\text{rf}} |m - n| \gg \omega_1, \quad (11)$$

which implies that an appropriate time T to evaluate the integral in Eq. (10) is of the order $2\pi/\omega_1$. Rapidly oscillating terms in $V_{\text{IF}}(\eta, t)$, *viz.*, terms with periods that are short compared to $2\pi/\omega_1$, are effectively averaged to zero when integrated over T , while static terms are unchanged. Time dependent terms with periods of order $2\pi/\omega_1$ are more troublesome, but for now we approximate such terms, if present, by their time average as well.

Although $V_{\text{IF}}(\eta, t)$ may not commute with itself at all times, it is valid to approximate it by its time average provided its eigen-frequencies are large compared to the transition energies of $\mathcal{H}_{Q,\text{IF}}(\eta)$ [18,20,21]. In contrast to the high-field rotating frame case, $V_{\text{IF}}(\eta, t)$ cannot be written as a sum of the I_x , I_y , and I_z operators, nor can simple symbolic expressions for $V_{\text{IF}}(\eta, t)$ be derived by hand, especially for $I > 3/2$. The most direct way to obtain $\bar{V}_{\text{IF}}(\eta)$ therefore is to explicitly evaluate $V_{\text{IF}}(\eta, t)$ in an appropriate basis set and integrate individual matrix elements according to Eq. (10).

We note that in the usual high field analysis, it is straightforward to recognize and remove time-dependent terms in $V_{\text{IF}}(\eta, t)$ without actually evaluating the integral in Eq. (10). However, the integration gives an equivalent result and provides a prescription for eliminating time-dependent terms that can be conveniently implemented with symbolic mathematical software.

If we accept the validity of Eq. (10), then $\mathcal{H}_{\text{IF}}(\eta, t)$ becomes piecewise constant during sequences of pulses and delays, and the density operator in the interaction representation, $\rho_{\text{IF}}(t)$, can be evaluated for periods

both with and without the rf field. The NQR observable for a solenoidal detector is magnetic dipole radiation, which means that the time domain signal will have the form:

$$S(t) = \text{Tr}\{\rho_{\text{IF}}(t)[\mathbf{I}_{\text{IF}}(t) \cdot \mathbf{n}]\}. \quad (12)$$

In the following examples, we assume that the initial condition corresponds to a high-temperature thermal equilibrium described by a reduced interaction frame density operator with the approximate form:

$$\rho_{\text{IF}}(0) \approx -\mathcal{H}_Q/ZkT, \quad (13)$$

where Z is the canonical partition function. The interaction frame observable is defined by the operator:

$$\mathbf{I}_{\text{IF}}(t) \cdot \mathbf{n} = U_{\text{IF}}^\dagger(\eta, t)\mathbf{I} \cdot \mathbf{n}U_{\text{IF}}(\eta, t). \quad (14)$$

To obtain the real and imaginary parts of the usual demodulated phase-sensitive signal at audio frequencies, the signal function represented by Eq. (12) must be multiplied by $\cos \omega_{\text{rf}}t$ and $\sin \omega_{\text{rf}}t$, respectively, and the sum frequency discarded.

3. Results and discussion

3.1. Nutation spectroscopy

3.1.1. $I = 3/2$

NQR nutation curves can be computed with the equations obtained in the preceding section for comparison with the exact solutions derived by Pratt et al. [4] for $I = 3/2$

(Fig. 1). Whereas Pratt et al.'s equation is valid for a stationary laboratory frame, the signal amplitude shown by the red curve in Fig. 1 is assumed to be detected in the interaction frame defined by the operator in Eq. (4). The nutation signal calculated with the exact solution is therefore an amplitude modulated sinusoid at the frequency of the observed transition, while the signal in the interaction representation is an oscillatory function at the offset frequency but with the same amplitude envelope. The rapidly oscillating term underneath the envelope is the real part of the detected signal. At all values of offset calculated the two show near-perfect agreement.

3.1.2. Extracting NQR parameters from nutation lineshapes

It has been previously demonstrated that the two independent parameters characterizing the EFG tensor can be determined from nutation powder lineshape measurements of a single NQR transition [5]. While this technique is particularly useful for NQR spectra that contain only a single resonance, it could also prove a more facile experimental method for obtaining EFG tensors than searching for the additional transitions in NQR spectra with widely spaced lines. Closed form expressions for nutation lineshapes have been derived for comparison with experimental data for nuclei with $I \leq 3/2$, but not for higher spins.

The nutation lineshape was shown by Harbison et al. to be strongly affected by the RF field inhomogeneity, spectrometer frequency offset, and relaxation processes.

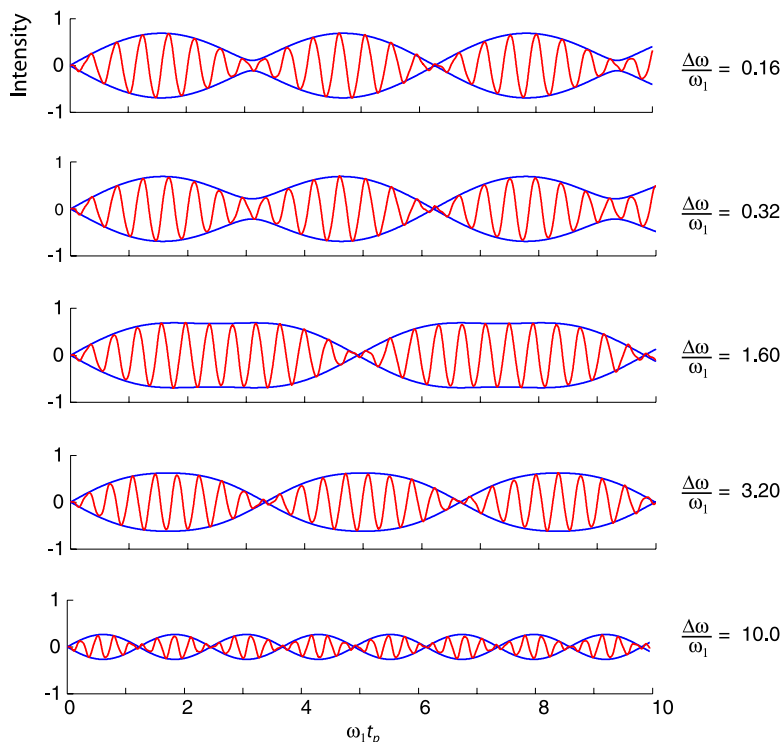


Fig. 1. Comparison of nutation curves of Pratt et al. (blue) with the numerical simulation in the interaction representation (red) for $\eta = 1$ at different values of the RF offset, $\Delta\omega$. For clarity, the blue time domain signal has been demodulated so the only time dependence shown is the amplitude modulation. The coil axis is assumed to lie along x with respect to the EFG PAS.

Velikite et al. [19] analyzed nutation lineshapes for on-resonance excitation, and obtained an empirical formula for determination of the asymmetry parameter from the NQR nutation frequency singularities. Using the methods outlined in previous sections, we have computed nutation curves for the transition of a spin-5/2 powder sample with $\eta = 0.5$ for on- and off-resonance excitation. The results for $\Delta\omega/\omega_1 = 0.5$ and $\Delta\omega/\omega_1 = 0.25$ (Fig. 2) illustrate the strong dependence of the lineshape on the offset of the carrier frequency from the NQR transition. Similar results are found for the lineshape dependence on RF inhomogeneity. Clearly, the error in determinations of the EFG tensor by this method is potentially large if such effects are not taken into account in the lineshape simulations.

3.2. Perturbation theory approximation and selection rules

The NQR transition moment obtained by stationary perturbation theory assuming a weak, on-resonance field of the form in Eq. (3) is:

$$F(\eta, \theta, \phi) \propto |\langle \psi_m(\eta) | \mathbf{I} \cdot \mathbf{n} | \psi_n(\eta) \rangle|^2. \quad (15)$$

Since, \mathcal{H}_Q connects only $|m\rangle$ states differing by an even number, its eigenstates $|\psi_m(\eta)\rangle$ in general will be a linear superposition of the I_z eigenstates $|m \pm k\rangle$, where k is an even number. It follows that $F(\eta, \theta, \phi)$ will be non-zero if and only if $|m - n|$ is an odd number.

The perturbation theory approximation of the transition moment exemplified by Eq. (15) is compared in Fig. 3 with the time-domain signal intensity calculated numerically according to the methods described in Section 2 for the case of $I = 7/2$, $\eta = 0.5$. The detection coil is assumed to lie along the x -axis of the EFG principal axis system. The spectra obtained by the two approaches are in close quantitative agreement. The relative transition amplitudes for both calculation methods are in good qualitative agree-

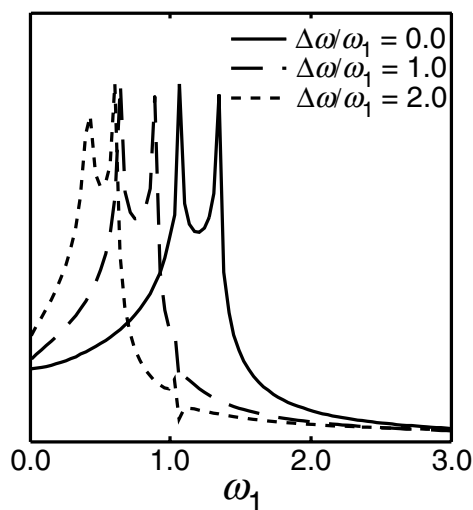


Fig. 2. On- and off-resonance nutation lineshapes for the spin-5/2 $|\psi_{\pm 3/2}\rangle \leftrightarrow |\psi_{\pm 1/2}\rangle$ NQR transition. The intensity scales of the spectra are individually normalized.

ment. The only transitions with non-vanishing intensity observed in the numerical spectrum correspond to $|m - n|$ an odd number, in agreement with the selection rule predicted from Eq. (15). The $|\psi_{\pm 7/2}\rangle \leftrightarrow |\psi_{\pm 3/2}\rangle$ transition is not seen in the full calculation, but this is likely due to its low probability.

3.2.1. Powder and single crystal spectra

The signal of an orientationally disordered sample is computed as an average of signals from a weighted cross section of orientations:

$$S_{\text{powder}}(\eta) = \int_0^{2\pi} \int_0^\pi S(\eta, \theta, \phi) \sin \theta d\theta d\phi. \quad (16)$$

Again, we take as an example the $I = 7/2$ case; other values of I display similar behavior. The signal intensity shows a strong dependence on the orientation of the coil axis relative to the EFG tensor of the quadrupole nuclei, especially at larger values of the asymmetry parameter. Therefore, it is expected that powder averages at large values of η will affect the signal intensity appreciably when compared to single crystals.

Fig. 4 compares the signal for the $|\psi_i\rangle \leftrightarrow |\psi_j\rangle$ transition for a powder versus a single crystal in which the coil is oriented along the x - and y -axis of the EFG coordinate system.

The maximum signal intensity for a single crystal always occurs when the coil is oriented along the x -axis of the EFG tensor, i.e., when $\theta = \pi/2$ and $\phi = 0$. It is not surprising that powder averaging loses signal intensity when compared to a single crystal in such cases. For non-zero values of the asymmetry parameter the coil orientation plays an important factor in the signal intensity as can be seen from Fig. 5. Therefore, at the signal minimum which occurs when the coil is oriented along the y -axis of the EFG tensor, signal is actually lost in the case of single crystals compared to the corresponding powder for η larger than about 0.1 – 0.5, depending on the specific transition.

3.3. Transient response to modulated rf fields

The performance of frequency-modulated pulses have been calculated numerically for spin-3/2 nuclei, but not for higher order spins [22]. Here, we illustrate the principles and value of the theoretical approach outlined in Section 2 with a study of the transient NQR response of an $I = 9/2$ spin system to a shaped pulse.

For purposes of demonstration, we assume the amplitude of the exciting pulse is given by a hyperbolic secant function

$$\omega_1(t) = \bar{\omega}_1 \text{sech}(t - t_0), \quad (17)$$

where ω_0 is set to the transitions, $|\psi_{\pm 7/2}\rangle \leftrightarrow |\psi_{\pm 1/2}\rangle$ and $|\psi_{\pm 9/2}\rangle \leftrightarrow |\psi_{\pm 3/2}\rangle$, at $\eta = 1$. For the amplitude- and phase-modulated pulse the phase was set to vary quadratically with time, resulting in a linear chirp. The results are shown in Fig. 6.

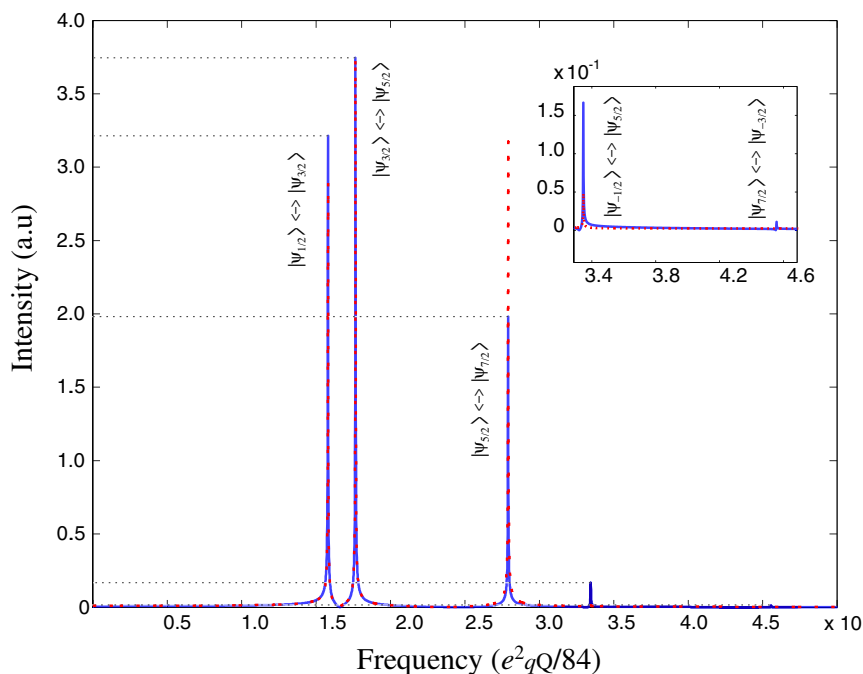


Fig. 3. Comparison of spectra for transition moment (solid blue line) and full calculations (dashed red line) for spin-7/2 with $\eta = 0.5$. Inset shows forbidden transition amplitudes. Pulse lengths for the main transitions was kept constant and halved for the $|\psi_{\pm 1/2}\rangle \leftrightarrow |\psi_{\pm 5/2}\rangle$ transition.

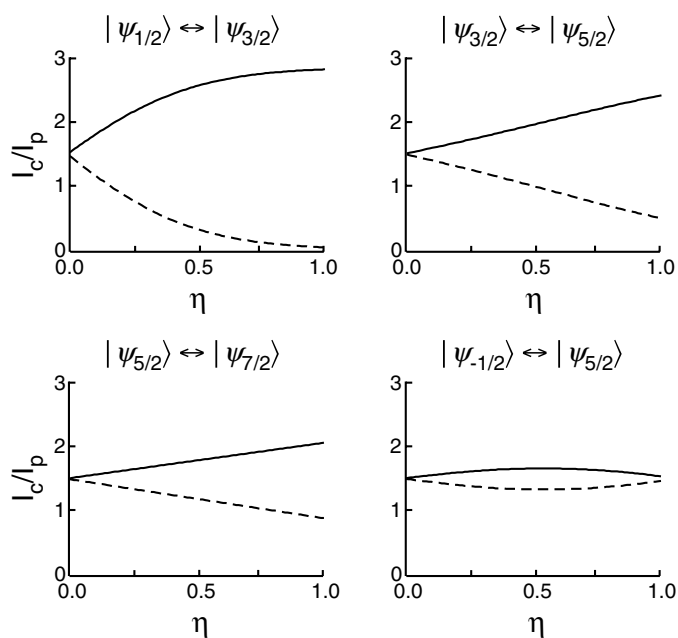


Fig. 4. Comparison of powder and single crystal signal intensities at different values of η for all observed spin-7/2 NQR transitions. Solid and dashed lines signify detection of the single crystal sample is with the coil along the x- and y-axes of the EFG tensor, respectively.

The intensity of the pulse is decreased by a factor of about 1/3 when phase modulation is added and rapidly oscillating terms are observed in the nutation curve. Such simulations can be helpful in determining the effects of pulse sequences on the signal intensity before

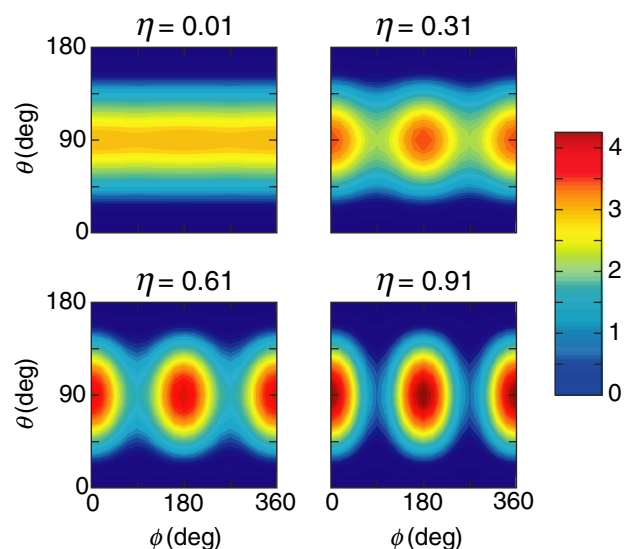


Fig. 5. Dependence of the signal amplitude on the orientation of the coil axis relative to the EFG PAS for spin-7/2 at different values of $0 \leq \eta \leq 1$ for the $|\psi_{\pm 5/2}\rangle \leftrightarrow |\psi_{\pm 3/2}\rangle$ transition. θ and ϕ are the polar and azimuthal angles, respectively.

performing experiments. For simplicity, relaxation is ignored.

4. Conclusion

Informative and useful NQR measurements can be made in the time domain that would not be possible

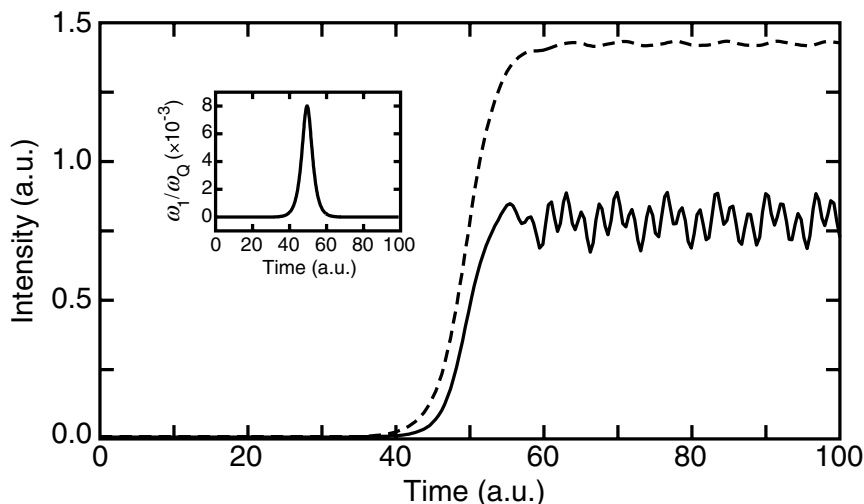


Fig. 6. Transient response of spin-9/2 nuclei with $\eta = 1$ to amplitude-modulated only (dash line) and amplitude- and phase-modulated (solid line) pulses. Inset: hyperbolic secant pulse shape.

in a frequency domain experiment. The theoretical framework developed here provides general guidance for the quantitative analysis of such experiments. The validity and versatility of this approach has been demonstrated by comparisons with perturbation theory calculations and the exact results for the special case of $I = 3/2$ spins.

The definition of the interaction representation and the discarding of non-secular terms in the interaction frame closely resembles the rotating frame approximations of high-field NMR spectroscopy. Unlike the simpler high-field case however, explicit time-averaging is required to identify and eliminate non-resonant time dependent terms, as exemplified by Eq. (10). This approximation may be refined by recognizing this expression as the zeroth order term of the Magnus expansion, and adding higher-order corrections [20,21]. In this way, even more complicated problems, such as those involving simultaneous excitation of multiple transitions, may also be treated. Furthermore, the method employed here is suitable for Zeeman perturbed NQR and other situations where interactions are small compared to the quadrupolar splitting [23].

5. Supporting information

Simulation programs for the Matlab platform are available at the US Department of Energy's ESTSC website <http://www.osti.gov/estsc/>.

Acknowledgments

We thank J. Granwehr and E. L. Hahn for helpful discussions. E.H. is supported by a fellowship from the US Department of Homeland Security under DOE contract number DE-AC05-00OR22750. The Pacific Northwest National Laboratory is operated for the US Department

of Energy by the Battelle Memorial Institute under Contract No. DE-AC05-76RLO1830.

References

- [1] T.P. Das, E.L. Hahn, Nuclear Quadrupole Resonance Spectroscopy, Academic, New York, 1958.
- [2] R.V. Pound, Nuclear electric quadrupole interactions in crystals, Phys. Rev. 79 (1950) 685–702.
- [3] M.H. Cohen, Nuclear quadrupole spectra in solids, Phys. Rev. 96 (1954) 1278–1284.
- [4] J.C. Pratt, P. Raghunathan, C.A. McDowell, Transient response of a quadrupolar spin system in zero applied field, J. Magn. Reson. 20 (1975) 313–327.
- [5] G.S. Harbison, A. Slokenbergs, T.M. Barbara, Two-dimensional zero-field nutation nuclear quadrupole resonance spectroscopy, J. Chem. Phys. 90 (1989) 5292–5298.
- [6] H. Robert, D. Pusiol, One-dimensional nutation nuclear quadrupole resonance spectroscopy for measurement of the electric field gradient tensor-asymmetry parameter, J. Chem. Phys. 106 (1997) 2096–2100.
- [7] S. Levy, A. Keren, Pure nuclear quadrupole resonance determination of the electric field gradient asymmetry for broad lines, J. Magn. Reson. 167 (2004) 317–321.
- [8] Y. Xia, C. Ye, NQR spectroscopy of powder sample with spin $I = 1$ and $3/2$ (I), Progr. Nat. Sci. 6 (1996) 284–292.
- [9] Y. Xia, Y. Shi, C. Ye, NQR spectroscopy of powder sample with spin $I = 1$ and $3/2$ (II), Progr. Nat. Sci. 6 (1996) 415–421.
- [10] Y.K. Lee, Spin-1 nuclear quadrupole resonance theory with comparisons to nuclear magnetic resonance, Concepts Magn. Reson. 14 (2002) 155–171.
- [11] N.E. Aïnbindler, G.B. Furman, Theory of multipulse averaging for spin systems with arbitrary nonequidistant spectra, Sov. Phys. JETP 58 (1983) 575–581.
- [12] D.J. Isbister, M.S. Krishnan, B.C. Sanctuary, Use of computer algebra for the study of quadrupole spin systems, Mol. Phys. 86 (1995) 1517–1535.
- [13] S.Z. Ageev, B.C. Sanctuary, Selective excitation of single and multiple quantum transitions for spin-7/2 in NQR, Mol. Phys. 87 (1996) 1423–1438.
- [14] J.-H. Wang, M.-Y. Liao, Sensitivity enhanced nuclear quadrupole correlation spectroscopy: application of single transition operators in nuclear quadrupole resonance of half-integer nucleus, J. Chem. Phys. 116 (2002) 3270–3276.

- [15] A. Ramamoorthy, Analysis of the performance of a phase alternated multiple pulse sequence in spin $I = 7/2$ zero-field NQR spectroscopy, *Mol. Phys.* 92 (1997) 1035–1038.
- [16] S.A. Smith, T.O. Levante, B.H. Meier, R.R. Ernst, Computer simulations in magnetic resonance. An object-oriented programming approach, *J. Magn. Reson.* 106 (1994) 75–105.
- [17] M. Bak, J.T. Rasmussen, N. Chr. Nielsen, SIMPSON: a general simulation program for solid-state NMR spectroscopy, *J. Magn. Reson.* 147 (2000) 296–330.
- [18] C.P. Slichter, *Principles of Magnetic Resonance*, 3rd ed., Springer, New York, 1990.
- [19] N. Velikite, N. Sinyavsky, M. Mackowiak, Lineshape analysis of 2D NMR and NQR nutation spectra of integer and half-integer quadrupolar nuclei, *Z. Naturforsch. A* 54 (1999) 351–357.
- [20] W. Magnus, On the exponential solution of differential equations for a linear operator, *Commun. Pure Appl. Math.* 7 (1954) 649–673.
- [21] P. Pechukas, J.C. Light, On the exponential form of time-displacement operators in quantum mechanics, *J. Chem. Phys.* 44 (1966) 3897–3912.
- [22] C. Schurrer, S.C. Perez, Performance of frequency-modulated pulses in NQR, *Appl. Magn. Reson.* 16 (1999) 135–146.
- [23] C. Dean, Zeeman splitting of nuclear quadrupole resonances, *Phys. Rev.* 96 (1954) 1053–1059.